다중척도 정칙화 방법을 이용한 영상복원

Multiscale Regularization Method for Image Restoration

이 남 용*
Nam-Yong Lee*

요 약

이 논문에서는 중복된 웨이블렛 변환영역에서 다중척도 정칙화를 이용한 새로운 영상복원방법을 제시하였다. 제안된 방법은 중복된 웨이블렛 변환을 이용하여 단일척도 영상복원문제를 다중척도의 영상복원문제로 변환한 후에, 각 척도에 의존하는 정칙화 방법을 이용하여 각 척도별로 영상복원을 하고 그 결과를 중복 웨이블렛 역변환을 통해 최종적인 영상복원을 얻는 방법이다. 제안된 방법은 웨이블렛 관련 복원부분에서는 다소 적은 정칙화 계수를 적용하여 뚜렷한 경계를 복원하는 반면, 적은 정칙화 계수에 적용한 것에 의해 발생하는 잡음은 웨이블렛 축소법을 이용하여 제거하였다. 제안된 방법의 향상된 영상복원 성능은 전통적인 Wiener 필터링과의 비교실험을 통해 검증하였다.

ABSTRACT

In this paper we provide a new image restoration method based on the multiscale regularization in the redundant wavelet transform domain. The proposed method uses the redundant wavelet transform to decompose the single-scale image restoration problem to multiscale ones and applies scale dependent regularization to the decomposed restoration problems. The proposed method recovers sharp edges by applying rather less regularization to wavelet related restorations, while suppressing the resulting noise magnification by the wavelet shrinkage algorithm. The improved performance of the proposed method over more traditional Wiener filtering is shown through numerical experiments.

Key words : Image restoration, wavelet shrinkage, multiscale regularization

I. Introduction

Mathematically, image restoration problem can be written as

$$y = p * f + z, \qquad (1)$$

where $p*f$ is the two dimensional convolution of p and f, y is an observed image, and p is the point spread function that represents the imaging system characteristic causing the blurring. In this paper, we consider additive white noise z as noise model. In most cases, because of the blurring effect by the point spread function p, the resulting image restoration problem is ill-posed in a sense that small perturbations in observed images can result in severe artifacts in restored images. Such instability is often overcome by the use of a regularization method, which is commonly done by imposing smoothing restriction on the image to be restored; the regularized image $\tilde{f}$ for the restoration problem is defined as the minimizer of

$$\|y - p * \phi\|^2 + \lambda \|S\phi\|^2,$$

where S is a smoothing transform. The parameter λ acts as a balancing parameter; if λ is large, then

*인제대학교 컴퓨터응용과학부
접수 일자 : 2004. 2. 06 수정 완료 : 2004. 5. 29
논문 번호 : 2004-1-5
※본 연구는 2002년도 인제대학교 학술연구조성비의 보조에 의해 수행되었음.

necessarily $\|S\phi\|^2$ must be small, thus the regularized image tends to be smoother, while when λ is small, then one can achieve a better-fitted but rough image.

While the restored images by regularization are likely to be less sensitive to noise, standard regularization methods that confine the restored image with a single overall restriction tends to lose edge information [1]. In order to overcome this problem, many spatially adaptive regularization methods have recently been developed with the purpose to provide simultaneously good noise removal in the smooth area and less smoothing in the edge area. Among those methods, Geman and Yang [2] used the half quadratic regularization method that addresses the nonlinear optimization problem. In Rudin et. al. [3] the regularization term is set to be $\|\phi\|_{BV}$, the total variation. In their approach, formation of edges is encouraged to make total variation of the restored image small. As a result the restored images look sharper than those obtained by conventional methods such as Wiener filtering, especially when the original image is piecewise constant.

There has been a significant trend in recent research regarding the use of the wavelet transform to the image restoration problem. The increased interest in this field is mainly due to the wavelet-based multiscale structure. The wavelet shrinkage method by Donoho and Johnstone [4], which shrinks the wavelet coefficients of noisy observed image towards zero, has been used to the various Gaussian noise removal problems [5], [6], etc. Several wavelet approaches have also been successfully applied to the tomographic reconstruction problems [7], [8], [9], [10], where the observed data, which are called projections, are noisy Radon transform of the image.

As mentioned earlier, the inversion process required in the image restoration is highly unstable, and various methods have been used to overcome resulting difficulties. The well-known Wiener filtering applies some filtering to the observed image before the actual inversion takes place, and the form of filters is easily determined by the decoupling property of the convolution in the Fourier transform domain. To use the wavelet transform effectively in the image restoration, we must have a fast and stabilized algorithm in computing the wavelet transform of the restored image from that of the observed image. But with the traditional wavelet transform, which has the downsampling in each decomposition step, it is impossible to have such algorithm.

In this paper we propose a new image restoration method based on the redundant wavelet transform. The redundant wavelet transform decouples the convolution at the expense of the redundancy in its image representation. Our approach begins with a rather smooth regularization for the coarsest scaling coefficients, and then a quite rough scale-dependent regularization for the remaining redundant wavelet coefficients. In our method the noise in the restored redundant wavelet coefficients is suppressed by the wavelet shrinkage.

Our work is motivated by Zervakis et al. [11], where the redundant wavelet transform is used to decouple the convolution as the proposed method of this paper, but, instead of the regularization method, the Wiener filtering is separately applied to the redundant wavelet coefficients at each scale. The Wiener filtering, however, whether it is single-scale or multi-scale, is restricted in use since it requires the original power spectrum and the adaptive implementation is not easy. Our method does not have these described difficulties.

We provide experimental results of the proposed method, the traditional Wiener filtering, and the multiscale Wiener filtering. The results show that the proposed method gives smaller errors than Wiener filtering for most images with various blurring factors and noise intensities except for some smooth images that are more contaminated by the noise than by the blurring. They also show that the restored images by the proposed method have less ringing effects and better perceptual image quality than those by Wiener filtering.

Other wavelet-based image restoration methods can be found in [12], [13], [14], etc. In Belge et al. [12], they used the wavelet shrinkage algorithm derived from the generalized Gaussian modeling on the wavelet coefficients. In Lee and Paik [13], to have a space-frequency adaptive image restoration by the Wiener filtering, the filter is separately determined in each band, where the band is generated by the traditional wavelet transform. In Banham et al. [1], [14], they used the Kalman filtering for the image restoration by utilizing the statistical similarity between in inter-scale wavelet coefficients.

This paper is organized as follows. In Section 2 we briefly explain the redundant wavelet representation of images. In Section 3 we propose a multiscale image restoration method. The performances of the proposed

method is shown in Section 4. Finally, discussion and conclusion are given in Section 5.

II. Redundant Wavelet Representation

In this section we present necessary concept of the basic wavelet theory needed for the presentation of this paper. For more details, see, e.g., [15].

Wavelets are defined by low pass filter (h_n) and high pass filter (g_n). The redundant wavelet transform and its inverse transform for images can be defined by the convolution with the tensor product of two one dimensional filters: To be specific, an image $f=(f_{n_1,n_2})$, let the finest coefficients $C^0_{n_1,n_2}$ be f_{n_1,n_2}. The redundant wavelet transform of the image f is obtained by successively applying the two dimensional convolutions

$$C^{k+1}=(\bar{h}\otimes\bar{h})*C^k, \qquad D^{k+1,1}=(\bar{h}\otimes\bar{g})*C^k$$
$$D^{k+1,2}=(\bar{g}\otimes\bar{h})*C^k, \qquad D^{k+1,3}=(\bar{g}\otimes\bar{g})*C^k,$$

where the convolution with the tensor product $u\otimes v$ is defined by

$$[(u\otimes v)*f]_{j_1,j_2}=\sum_{n_1,n_2} u_{j_1-n_1}v_{j_2-n_2}f_{n_1,n_2}$$

and $\bar{h}_n=h_{-n}$ $\bar{g}_n=g_{-n}$. The two dimensional inverse redundant wavelet transform reconstructs the original image C^0 from $D^{1,\varepsilon}, D^{2,\varepsilon}, \cdots, D^{k_0,\varepsilon}, C^{k_0}$, $\varepsilon=1,2,3,$ by successively using

$$C^k=\frac{1}{4}[(h\otimes h)*C^{k+1}+(h\otimes g)*D^{k+1,1}$$
$$+(g\otimes h)*D^{k+1,2}+(g\otimes g)*D^{k+1,3}].$$

The redundant wavelet coefficients C^k, $D^{k,\varepsilon}$, $\varepsilon=1,2,3,$ are generated from the successive convolutions of f with tensor products $(\bar{h}\otimes\bar{h})$, $(\bar{h}\otimes\bar{g})$, $(\bar{g}\otimes\bar{h})$, or $(\bar{g}\otimes\bar{g})$. Thus the redundant wavelet transform can commute with the convolution, i.e.,

$$C^k(p*f)=p*C^k(f) \tag{2}$$

and

$$D^{k,\varepsilon}(p*f)=p*D^{k,\varepsilon}(f), \tag{3}$$

where we have used the notations $C^k(f)$ and $D^{k,\varepsilon}(f)$ to denote the k-th redundant scaling coefficients and the k-th redundant wavelet coefficients of f, respectively.

III. Multiscale Regularization

Let us consider the minimizer $\tilde{f}$ of the following functional to the image restoration problem (1):

$$\|y-p*\phi\|^2+\lambda\|\phi\|^2.$$

Then it is not difficult to show that the minimizer image $\tilde{f}$ is the convolution of the observed image y with

$$q=F^{-1}\left(\frac{P^*_{n_1,n_2}}{|P_{n_1,n_2}|^2+\lambda\ \mathbf{1}_{n_1,n_2}}\right)$$

where F is the Fourier transform, $P=F(p)$, and $\mathbf{1}_{n_1,n_2}$ is the all 1 matrix.

While the regularized restorations are likely to be less sensitive to noise, the regularization methods based on the overall restriction on the restored image tends to result in either the loss of edge information or the poor noise removal. For instance, the restored images associated with a large λ can have a good noise removal property, but it often loses the edge information. On the other hand, the restored images with a small λ are likely to suffer from the poor noise removal, while they might provide a sharp restoration of edges.

To overcome the described difficulty, in this paper we suggest a multiscale restoration method. The proposed method is based on the regularization and the wavelet shrinkage techniques on the redundant wavelet transform domain. By applying the redundant wavelet transform, we change the single-scale image restoration problem (1) to the multiscale image restoration problems

$$C^{k_0}(y)=p*C^{k_0}(f)+C^{k_0}(z) \tag{4}$$

and

$$D^{k,\varepsilon}(y)=p*D^{k,\varepsilon}(f)+D^{k,\varepsilon}(z),$$

for $1\le k\le k_0$, $\varepsilon=1,2,3.$

In the proposed method we apply the regularization techniques to the restoration problems related to the redundant wavelet coefficients and then use the wavelet shrinkage algorithm to suppress the noise in the restored redundant wavelet coefficients. In our approach, we wish to approximate the true coarsest

scaling coefficients $C^{k_0}(f)$ rapidly by the regularized solution in (4) and remove most of noises in the restored redundant wavelet coefficients by using the wavelet shrinkage algorithm, while preserving an important image feature such as edges.

We begin with the restoration problem associated with the coarsest scaling coefficients C^{k_0}, i.e.,

$$C^{k_0}(y)=p*\phi+C^{k_0}(z).$$

To solve this, we consider the following regularized solution

$$\mathcal{C}^{k_0}=\arg\min_{\phi}(\|C^{k_0}(y)-p*\phi\|^2+\lambda_{k_0}\|\phi\|^2).$$

We can easily compute the minimizer of the above functional by

$$\mathcal{C}^{k_0}=q_{k_0,0}*C^{k_0}(y)$$

where

$$q_{k_0,0}=F^{-1}\left(\frac{P^*_{n_1,n_2}}{|P_{n_1,n_2}|^2+\lambda_{k_0}\mathbf{1}_{n_1,n_2}}\right).$$

Once we compute the coarsest redundant scaling coefficients $\mathcal{C}^{k_0}$, we consider the following regularized solution

$$\mathcal{D}^{k,\varepsilon}=\arg\min_{\phi}(\|D^{k,\varepsilon}(y)-p*\phi\|^2+\lambda_{k,\varepsilon}\|\phi\|^2)$$

for $1\le k\le k_0$ and $\varepsilon=1,2,3$. With a similar argument, we have

$$\mathcal{D}^{k,\varepsilon}=q_{k,\varepsilon}*D^{k,\varepsilon}(y),$$

where

$$q_{k,\varepsilon}=F^{-1}\left(\frac{P^*_{n_1,n_2}}{|P_{n_1,n_2}|^2+\lambda_{k,\varepsilon}\mathbf{1}_{n_1,n_2}}\right).$$

The shrinkage operator S_μ is defined by

$$S_\mu(x)=\begin{cases}x-sign(x)\mu & \text{if } |x|>\mu\\ 0 & \text{if } |x|\le\mu\end{cases}$$

for $\mu>0$. We use the wavelet shrinkage algorithm to suppress the noise in the restored redundant wavelet coefficients $\mathcal{D}^{k,\varepsilon}$. Finally, we compute $\mathcal{C}^{k-1}$ from $\mathcal{C}^k$ and $S_{\mu_{k,\varepsilon}}(\mathcal{D}^{k,\varepsilon})$. We proceed the above steps until we get the restored image $\tilde{f}=\mathcal{C}^0$.

For the restored redundant wavelet coefficients, finding optimal parameters for $\lambda_{k,\varepsilon}$ and $\mu_{k,\varepsilon}$ simultaneously is very difficult. In this work we only consider the case where the shrinkage parameters are of the form

$$\mu_{k,\varepsilon}=\mu 2^{-k}$$

and the regularization parameters satisfy

$$\lambda_{k_0,0}=\lambda 2^{k_0} \quad \text{and} \quad \lambda_{k,\varepsilon}=\beta\lambda 2^{k}$$

with $0<\beta<1$. Roughly speaking, we believe that a better fitted image restoration with a smaller regularization parameters $\lambda_{k,\varepsilon}$ and then a noise removal with a larger shrinkage parameter to the finer redundant wavelet coefficients gives better results.

Before closing this section, we comment on the Wiener filtering method for the future use. As the restored image for the image restoration problem (1), the Wiener filtering provides

$$\tilde{f}=g*y \quad g=F^{-1}\left(\frac{S^{ff}_{n_1,n_2}P^*_{n_1,n_2}}{|P_{n_1,n_2}|^2S^{ff}_{n_1,n_2}+S^{zz}_{n_1,n_2}}\right),$$

where S^{ff} denotes the power spectrum of the random field f. Here we assume that the average intensities of true image f as random filed are 0 to simplify our presentation. In practice, we estimate S^{ff} by using y. As mentioned earlier, our method is similar to that of Zervakis et. al. [11]. They applied the Wiener filtering to the multiscale image restoration problem (2), (3), i.e.,

$$\mathcal{C}^{k_0}=q_{k_0,0}*C^{k_0}(y)$$

and

$$\mathcal{D}^{k,\varepsilon}=q_{k,\varepsilon}*D^{k,\varepsilon}(y),$$

where

$$q_{k_0,0}=F^{-1}\left(\frac{S^{C^{k_0}(f)C^{k_0}(f)}_{n_1,n_2}P^*_{n_1,n_2}}{|P_{n_1,n_2}|^2S^{C^{k_0}(f)C^{k_0}(f)}_{n_1,n_2}+S^{C^{k_0}(z)C^{k_0}(z)}_{n_1,n_2}}\right)$$

and

$$q_{k,\varepsilon}=F^{-1}\left(\frac{S^{D^{k,\varepsilon}(f)D^{k,\varepsilon}(f)}_{n_1,n_2}P^*_{n_1,n_2}}{|P_{n_1,n_2}|^2S^{D^{k,\varepsilon}(f)D^{k,\varepsilon}(f)}_{n_1,n_2}+S^{D^{k,\varepsilon}(z)D^{k,\varepsilon}(z)}_{n_1,n_2}}\right)$$

for $1\le k\le k_0$ and $\varepsilon=1,2,3$. Again, we use the observed image y in estimating statistical terms related to f.

IV. Simulations

We conducted image restoration experiments with the proposed method(MW), which uses multiscale regularization and wavelet shrinkage techniques, the traditional single-scale Wiener filtering(SF), and the multiscale Wiener filtering(MF) by Zervakis et. al. [11] to the image that is blurred by the point spread function

$$p_{n_1, n_2} = \frac{1}{\sqrt{\pi}\alpha} e^{-\frac{n_1^2 + n_2^2}{\alpha^2}} \quad (5)$$

and then contaminated by the white noise

$$z_{n_1, n_2} \sim G(0, \sigma^2). \quad (6)$$

Our main conclusion is that the proposed restoration method MW provides smaller errors in terms of the peak signal-to-noise ratio(PSNR)

$$\text{PSNR} = 10 \log_{10} \left(\frac{255^2}{N^2 \sum_{i,j} |f_{i,j} - \tilde{f}_{i,j}|^2} \right)$$

where $f_{i,j}$ and $\tilde{f}_{i,j}$ are the (i, j) pixels in the original and restored images, respectively, and the size of image is $N \times N$, and gives sharper edges and less ringing effects than SF and MF do.

Table 1. PSNRs by the proposed method(MW) with $\lambda = 0.01$, $\beta = 0.6$, $\mu = \sqrt{2 \log N^2}\sigma$, and the wavelet depth $k_0 = 3$.

α	0.03 N			0.04 N			0.05 N		
σ	2.0	3.0	4.0	2.0	3.0	4.0	2.0	3.0	4.0
Baboon	20.77	20.66	20.54	20.19	20.15	20.08	19.87	19.83	19.80
Butterfly	26.12	25.82	25.52	23.70	23.61	23.46	21.94	21.89	21.81
Cameraman	25.22	24.99	24.72	23.70	23.59	23.44	22.73	22.67	22.62
Woman	25.36	25.12	24.83	24.37	24.24	24.06	23.67	23.59	23.50
Lenna	26.39	26.11	25.72	25.00	24.84	24.67	24.02	23.94	23.84
Peppers	27.40	27.06	26.60	25.89	25.74	25.54	24.75	24.66	24.55
Barbara	27.11	26.76	26.31	26.22	26.04	25.78	25.39	25.28	25.13
Couple	30.18	29.56	28.81	28.69	28.39	28.01	27.68	27.53	27.25
Girl	31.11	30.36	29.51	29.57	29.20	28.69	28.31	28.13	27.88
Bird	32.55	31.48	30.35	30.98	30.44	29.72	29.54	29.29	28.97

Table 2. PSNRs by the single scale Wiener filtering(SF). The boldface is used to indicate the cases where SF outperforms MW.

α	0.03 N			0.04 N			0.05 N		
σ	2.0	3.0	4.0	2.0	3.0	4.0	2.0	3.0	4.0
Baboon	20.43	20.32	20.25	19.98	19.90	19.85	19.71	19.65	19.60
Butterfly	24.93	24.48	24.19	22.86	22.50	22.24	21.37	21.10	20.91
Cameraman	24.33	24.09	23.89	23.14	22.92	22.77	22.35	22.18	22.05
Woman	24.80	24.61	24.46	23.96	23.80	23.67	23.33	23.19	23.07
Lenna	25.54	25.28	25.06	24.35	24.15	24.01	23.57	23.38	23.25
Peppers	26.50	26.22	25.99	25.18	24.93	24.72	24.20	23.97	23.80
Barbara	26.60	26.40	26.22	25.71	25.50	25.35	24.92	24.73	24.57
Couple	29.20	28.87	28.64	27.97	27.68	27.50	27.02	26.80	26.62
Girl	30.18	29.78	29.48	28.61	28.31	28.09	27.60	27.35	27.17
Bird	31.92	31.49	31.12	30.16	29.77	29.49	28.86	28.52	28.33

Table 3. PSNRs by the multiscale Wiener filtering(MF). The boldface is used to indicate the cases where MF outperforms MW.

α	0.03 N			0.04 N			0.05 N		
σ	2.0	3.0	4.0	2.0	3.0	4.0	2.0	3.0	4.0
Baboon	20.61	20.50	20.43	20.12	20.05	20.00	19.82	19.77	19.72
Butterfly	25.63	25.23	24.99	23.55	23.23	22.97	21.93	21.68	21.47
Cameraman	24.76	24.53	24.34	23.52	23.33	23.16	22.66	22.51	22.41
Woman	25.10	24.93	24.77	24.26	24.10	23.98	23.60	23.46	23.35
Lenna	25.99	25.74	25.54	24.75	24.55	24.42	23.91	23.75	23.63
Peppers	26.95	26.71	26.48	25.64	25.41	25.23	24.63	24.40	24.25
Barbara	26.92	26.73	26.54	26.05	25.87	25.73	25.28	25.10	24.95
Couple	29.73	29.36	29.07	28.41	28.16	27.96	27.43	27.24	27.03
Girl	30.76	30.34	30.04	29.20	28.90	28.64	28.05	27.82	27.64
Bird	32.56	32.08	31.66	30.81	30.43	30.12	29.46	29.17	29.94

We use the piecewise constant biorthogonal wavelet filters with tap length 10. We modified the wavelets at the boundary in a way equivalent to making the image periodic. We set the depth k_0 of wavelet decomposition to be 3.

Fig. 1. Original image(Cameraman)

Fig. 2. Degraded by Gaussian blurring($\alpha = 0.04N$) and white noise($\sigma = 3.0$)

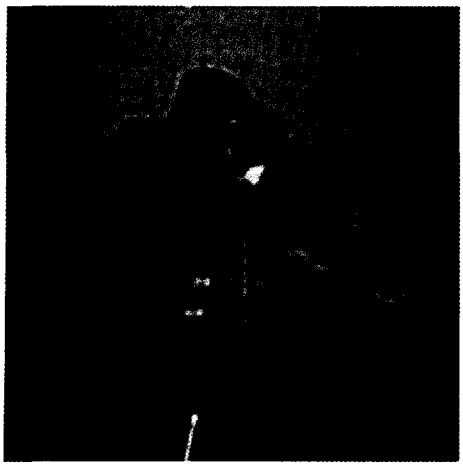

Fig. 3. Restored image by MW with $\lambda = 0.01$, $\beta = 0.6$, and $\mu = \sqrt{2 \log N^2}\sigma$

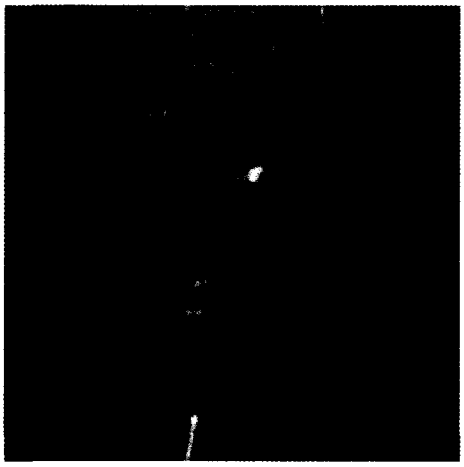

Fig. 4. Restored image by SF

Fig. 5. Restored image by MF

We used 10 standard 256-grey with $N = 256$ and several blurring factors $\alpha = 0.03N, 0.04N, 0.05N$ in (5) and noise intensities $\sigma = 2.0, 3.0, 4.0$ in (6). We chose 'Baboon', 'Butterfly', 'Cameraman', 'Woman', 'Lenna', 'Peppers', 'Barbara', 'Couple', Girl', 'Bird' in order from a large collection of test images to have varying high frequency energies(To measure this, we calculate the energy contained in the standard wavelet transform domain) in selected images. Here 'Baboon' has the largest high frequency energy and 'Bird' has the smallest one.

Table 1, 2, and 3 show the results of MW, SF, and MF experiments, respectively, with PSNRs of the restored images. For MW, we used $\lambda = 0.01$, $\beta = 0.6$, and $\mu = \sqrt{2 \log N^2}\sigma$. The parameters λ and β are selected as the experimental parameters from the test with 'Cameraman' image and then used for all other images. The experiments with other images indicates that it is better to use a larger λ for smoother or noisier images. We certainly believe that there is strong relation between the smoothness of images and the optimal parameters, but we shall not address this issue in this paper.

Fig. 6. Original image(Bird)

Fig. 7. Degraded by Gaussian blurring($\alpha = 0.04N$) and white noise($\sigma = 3.0$)

Fig. 8. Restored image by MW with $\lambda = 0.01$, $\beta = 0.6$, and $\mu = \sqrt{2 \log N^2 \sigma}$

Fig. 9. Restored image by SF

Fig. 10. Restored image by MF

In Table 2 and 3 we used the boldface to indicate the case where SF or MF outperform MW. As we can see from Table 1, 2, and 3, MW gives smaller errors in terms of PSNR than SF and MF for most images with most cases except for some smooth images that are more contaminated by the noise than by the blurring. Figure 1 and 6 show original image 'Cameraman' and 'Bird', and Figure 2 and 7 show noisy and blurred version of Figure 1 and Figure 6, respectively, with $\alpha = 0.04$ and $\sigma = 3.0$. Figure 3, 4, and 5 show the restored images by MW, SF, MF, respectively, from the noisy blurred image in Figure 2. Comparing the restored images by SF and MF with MW, sharper edges are obvious in MW. The textual pattern of the ground is a greater extent in Figure 4 and 5 than in Figure 3. This is due to the fact that SF and MF remove too much of high frequency information in those region while removing noises. Moreover, in MW some ringing effects around strong edges are greatly suppressed, for example, regions around legs of the tripod in 'Cameraman'. Figure 8, 9, and 10 show the restored images by MW, SF, MF, respectively, from the noisy blurred image in Figure 7.

As we can see from Figure 6, the image 'Bird' has very smooth background, and this is the region where MW has certain difficulty in removing noises. It is, however, obvious that MW provides sharper edges and less ringing effects than SF and MF for smooth images. With these rather subjective evidences and objective results in Table 1, 2, and 3, we conclude that the restored images by MW have less ringing effects and better perceptual image quality than those by SF and MF.

V. Conclusions

We used the PSNR measure to compare the performance of the proposed method(MW) with the traditional Wiener filtering(SF) and the multiscale Wiener filtering(MF)[11]. Through these simulation studies, we conclude that MW gives smaller errors than SF and MF for most images with most cases except for some smooth images that are more contaminated by the noise than by the blurring. We also conclude that the restored images by MW have less ringing effects and better perceptual image quality than those by SF and MF.

The improved performance of MW comes at expense of longer restoration time. The proposed method MW requires approximately same amount of computations as MF does, but, as compared with SF, it needs

approximately $3k_0+1$ times of that needed for SF plus $O(N^2 \log N)$ computations for images with $N \times N$ pixels. Due to rapid progress in computing environment, it is believed that the computing time in MW and MF would be no longer a big problem.

VI. References

[1] M. Banham and A. Katsaggelos.: 'Spatially Adaptive Wavelet-based Multiscale Image Restoration', IEEE Trans. Image Processing, Vol. 5, No. 4, pp. 619-634, 1996.

[2] D. Geman and C. Yang: 'Nonlinear Image Recovery with Half-Quadratic Regularization', IEEE Trans. Image Processing, Vol. 4, No. 7, pp. 932-946, 1995.

[3] L. Rudin, S. Osher, and E. Faemi: 'Nonlinear Total Variation based Noise Removal Algorithms', Physica D, Vol. 60, pp. 259-268, 1992.

[4] D. Donoho and I. Johnstone: 'Adapting to Unknown Smoothness via Wavelet Shrinkage', J. Amer. Statist. Assoc., Vol. 2, pp. 101-126, 1995.

[5] A. Chambolle, R. DeVore, N._Y. Lee, and B. Lucier: 'Nonlinear Wavelet Image Processing: Variational Problems, Compression, and Noise Removal through Wavelet Shrinkage', IEEE Trans. Image Processing, Vol. 7, No. 3, pp. 319-335, 1998.

[6] D. Donoho and I. Johnstone: 'Ideal Spatial Adaptation by Wavelet Shrinkage', Biometrika, Vol. 81, pp. 425-455, 1994.

[7] Y. Choi, J.-Y. Koo, and N.-Y. Lee: 'Image Reconstruction using the Wavelet Transform for Positron Emission Tomography', IEEE Trans. Medical Imaging, Vol. 20, No. 11, pp. 1188-1193, 2001.

[8] D. Donoho: 'Nonlinear Solution of Linear Inverse Problem by Wavelet-Vaguelette Decomposition', Appl. Comput. Harmon. Anal., Vol. 2, pp. 101-126, 1995.

[9] E. Kolaczyk: 'A Wavelet Shrinkage Approach to Tomographic Image Reconstruction', J. Amer. Statist. Assoc., Vol. 91, pp. 1079-1090, 1996.

[10] N.-Y. Lee and B. Lucier: 'Wavelet Methods for Inverting the Radon Transform with Noisy Data', IEEE Trans. Image Processing, Vol. 10, No. 1, pp. 79-94, 2001.

[11] M. Zervakis, T.M. Kwon, and J.-S. Yang: 'Multiresolution Image Restoration in the Wavelet Domain', IEEE Trans. Circuits Syst. II, Vol. 42, No. 9, pp. 578-591, 1995.

[12] M. Belge, M. Kilmer, and E. Miller: 'Wavelet Domain Image Restorations with Adaptive Edge-Preserving Regularization', IEEE Trans. Image Processing, Vol. 9, No. 4, pp. 597-608, 2000.

[13] H.H. Lee and J.K. Paik: 'Space-Frequency Adaptive Image Restoration based on Wavelet Decomposition', Proc. of IEEE Asia Pacific Conference on Circuits and Systems, Seoul, Korea, pp. 512-515, 1996.

[14] M. Banham, N. Galatsanos, H. Gonzalez, and A. Katsaggelos: 'Multichannel Restoration of Single Channel Images using a Wavelet-based Dub band Decomposition', IEEE Trans. Image Processing, Vol. 3, No. 6, pp. 821-833, 1994.

[15] I. Daubechies: 'Ten Lectures on Wavelets', SIAM, Philadelphia, 1992.

이 남 용(Nam-Yong Lee)
1990년 2월: 서울대 수학과 졸업
1997년 12월: Purdue University (Ph.D.)
2002년 9월 - 현재 : 인제대학교 컴퓨터응용 용과학부 전임강사